Hindawi
Journal of Advanced Transportation
Volume 2019, Article ID 4805613, 17 pages
https://doi.org/10.1155/2019/4805613

Research Article

A Two-Step Approach for Airborne Delay Minimization Using Pretactical Conflict Resolution in Free-Route Airspace

Ramazan Kursat Cecen[1] **and Cem Cetek**[2]

[1]*Anadolu University, Eskisehir, Turkey*
[2]*Eskisehir Technical University, Eskisehir, Turkey*

Correspondence should be addressed to Ramazan Kursat Cecen; ramazankursatcecen@anadolu.edu.tr

Received 27 November 2018; Accepted 6 March 2019; Published 1 April 2019

Guest Editor: Jesica de Armas

This study proposes a two-step solution approach for aircraft conflict resolution and fuel consumption due to resolution maneuver occurring in free-route airspace. This model aims to provide a mathematical basis for a decision-support system that is used during the pretactical conflict resolution in air traffic management. Mathematical model of the first step presents alternative entry points on both sides of existing sector entry points to minimize delays by directing aircraft to the most convenient entry points. The second step suggests a vector deflection maneuver to minimize extra fuel consumption caused by conflict resolution. GAMS/CPLEX solver is used to solve the first step of the model but the solution is not produced in a reasonable time. To obtain feasible solutions, genetic algorithm and tabu search algorithms are implemented in the first step. Small size test problems are generated to evaluate the metaheuristic algorithms, and results are compared with GAMS/CPLEX solver solutions. According to this comparison, both metaheuristics algorithms produce near optimal solutions in a reasonably short time. The proposed approach has made significant improvements for airborne delays and extra fuel consumption caused by aircraft conflicts resolution in large-scaled airspaces.

1. Introduction

Air transportation has evolved to be a global industry with its large-scaled, complex, and rapidly growing nature. It has a unique impact on commercial and economic growth not only because it provides rapid world-wide transportation critical for international business, trade, and tourism, but also because it facilitates regional economic and social growth. Airlines carried around 4.1 billion passengers with revenue passenger kilometers over 7.7 trillion as well as 6 trillion-US$-value of cargo in 2017 [1]. The total air traffic passenger demand has doubled in the last fifteen years, and 4.4% average annual growth is expected over the next twenty years [2]. This rapid growth in the demand overwhelms the current airspace capacities of air traffic management (ATM) system which is responsible for safe, efficient, and economic operations of flights within this global network. This imbalance between the capacity and demand leads to more airborne delays and congestions inducing increased operational costs, environmental impacts, customer dissatisfaction, and air traffic controllers' workload. Therefore, the improvement of the current airspace capacities is addressed as a critical issue for the sustainable growth of the industry in ICAO's long-term Global Air Navigation Plan [3] as well as European Union's Single European Sky ATM Research (SESAR) objectives [4].

Free-routing of aircraft is one of the effective methods to enhance airspace capacities as well as efficiency of flight operations based on the use of user-preferred trajectories. Free-route airspace (FRA) allows airlines to freely plan their flights between a defined entry and exit points without reference to the current air traffic service route networks while flights still oblige to follow the instructions of air traffic controllers [5]. Despite its advantages, FRA increases the traffic complexity and conflict detection due to the increase in the number of intersection points; therefore, the entire airspace becomes a potential "hot spot" [6]. Pretactical conflict detection and resolution (CDR) using improved decision-support systems can be one of the alternatives to handle this traffic complexity efficiently within FRAs.

Aircraft operating in the same airspace should maintain predefined safe separation distances between each other. These minimum separation distances are accepted as 5 nautical miles horizontally and 1000 feet vertically for en-route airspace. If air traffic controllers detect any loss of separation, they apply suitable conflict resolution maneuvers to aircraft in order to prevent any risk of collision. There are three main resolution maneuvers used for the collision avoidance between aircraft pairs: heading change, airspeed change, and flight level change. While heading and speed change maneuvers involve the adjustment of the direction or the magnitude of the airspeed vector in the horizontal plane, flight level change deals with climbing or descending aircraft in the vertical plane. Conflict resolution (CR) problem involves the search of one (or combination) of these maneuvers to ensure safe separation between aircraft. Numerous studies have proposed different mathematical models and approaches for CR problems, and detailed reviews were provided by Kuchar and Yang [7] and Martin-Campo [8]. Rodionova and Sridhar [9] classified these approaches as tactical (performed within 30 minutes prior to the conflict), pretactical (performed up to 2 hours prior to the conflict), and strategic (performed more than 2 hours prior to the conflict) CR problems.

This study addresses pretactical CR between aircraft pairs in the horizontal plane using heading change maneuvers within the time period of 20 to 60 minutes prior to the potential conflicts within the FRA. The model focuses on deterministic aircraft motion. A two-step approach is developed to minimize total airborne delay and extra fuel consumption per aircraft due to the required heading change resolution maneuver, respectively. The first step presents a mixed-integer linear optimization model along with two metaheuristics: genetic algorithms and tabu search, while the second step uses a nonlinear programming (NLP) model. Mixed-integer programming has been extensively applied to aircraft CDR problems. Pallottino et al. [10] developed two different mixed-integer linear models using either airspeed change or heading change resolution maneuvers. Christodoulou and Costoulakis [11] proposed a mixed-integer linear model combining these two resolution maneuvers for small-scale problems. Vela et al. [12, 13] presented mixed-integer linear models to minimize fuel burn using combined airspeed and altitude change resolutions and airspeed and heading angle change resolutions, respectively. Alonso-Ayuso et al. [14] introduced a mixed 0-1 linear optimization model resolving conflicts and returning aircraft to their original routes via airspeed and altitude changes. Later on Alonso-Ayuso et al. [15] also proposed two MILP models using just altitude change and combined altitude and airspeed changes. Cafieri and Durand [16] proposed a MINLP formulation allowing aircraft to change their airspeeds to avoid conflicts. Omer [17] formulated a MILP model using both airspeed and heading change based on space discretization of aircraft trajectories. Cafieri and Rey [18] proposed a MINLP model that adapts speed adjustment method to maximize the largest conflict free aircraft set. Besides these exact solution models, metaheuristics approaches such as genetic algorithm [19], ant colony optimization [20, 21], and particle swarm optimization [22] were presented to obtain good and feasible solutions in a short time; nonetheless they cannot guarantee globally optimal solution.

This study presents an alternative approach for pretactical CR based on flexible airspace entry point assignment which basically attempts to resolve conflict with no airborne delay by changing conflict geometries in the first step. The proposed approach ensures the safe separation using space discretization technique which allows us to focus on the critical points including entry, exit, and route intersection points instead of searching the whole airspace. The model checks all possible pairwise conflicts on trailing, crossing, merging, and diverging routes using these critical points. If any airborne delay is required to resolve aircraft conflicts, the second step searches a feasible vector deflection model corresponding to the airborne delay with minimum total fuel consumption per each aircraft before entering to the airspace. The vector deflection maneuver is a nonlinear model which includes the effects of bank angle changes as well as aerodynamic and propulsive characteristics on fuel consumption rate. The model determines bank angle, deflection angle, and vector maneuver distance within the lower and upper bounds to provide fuel optimal vector maneuver for the given airborne delay. The proposed two-step model aims to provide a mathematical basis for a decision-support system that can be used during pretactical control of flights in air traffic management and, therefore, metaheuristics are implemented to the first step of the model to obtain good and feasible solutions in a reasonable time.

2. Problem Statement

An airspace is any volume of the earth's atmosphere of defined dimensions which accommodates flights with or without air traffic control services. Airspaces can be classified as controlled, uncontrolled, and special airspaces according to air traffic services provided and flight requirements. Flight operations taking place in controlled airspaces receive air traffic control services according to the airspace types such as airport zones (CTR), terminal control areas (TMA), and en-route airspaces [23]. En-route airspaces cover the largest portion of the controlled airspace where flights in the climb, cruise, and descend phases are monitored and controlled by the relevant Area Control Center (ACC). The conventional en-route airspaces include a network of fixed waypoints and routes which aircraft have to follow during their flights. FRA, on the other hand, allows aircraft to choose their routes freely between the predefined airspace entry and exit points. Figure 1 presents a generic FRA with predefined boundaries, entry points (i.e., $EP_1, EP_2, \ldots, EP_k$), and exit points (i.e., $XP_1, XP_2, \ldots, XP_l$).

2.1. Flexible Entry Point Approach for FRA. This study adopts a flexible entry point approach which suggests adding two alternative entry points on both sides of the existing entry points with a certain distance (i.e., 10 NM), while preserving the existing boundaries and existing entry and exit points of FRA (Figure 2). Each existing entry point with its alternatives forms an entry area (i.e., $EA_1, EA_2, \ldots, EA_j$). This approach, therefore, enables aircraft to avoid all potential pairwise

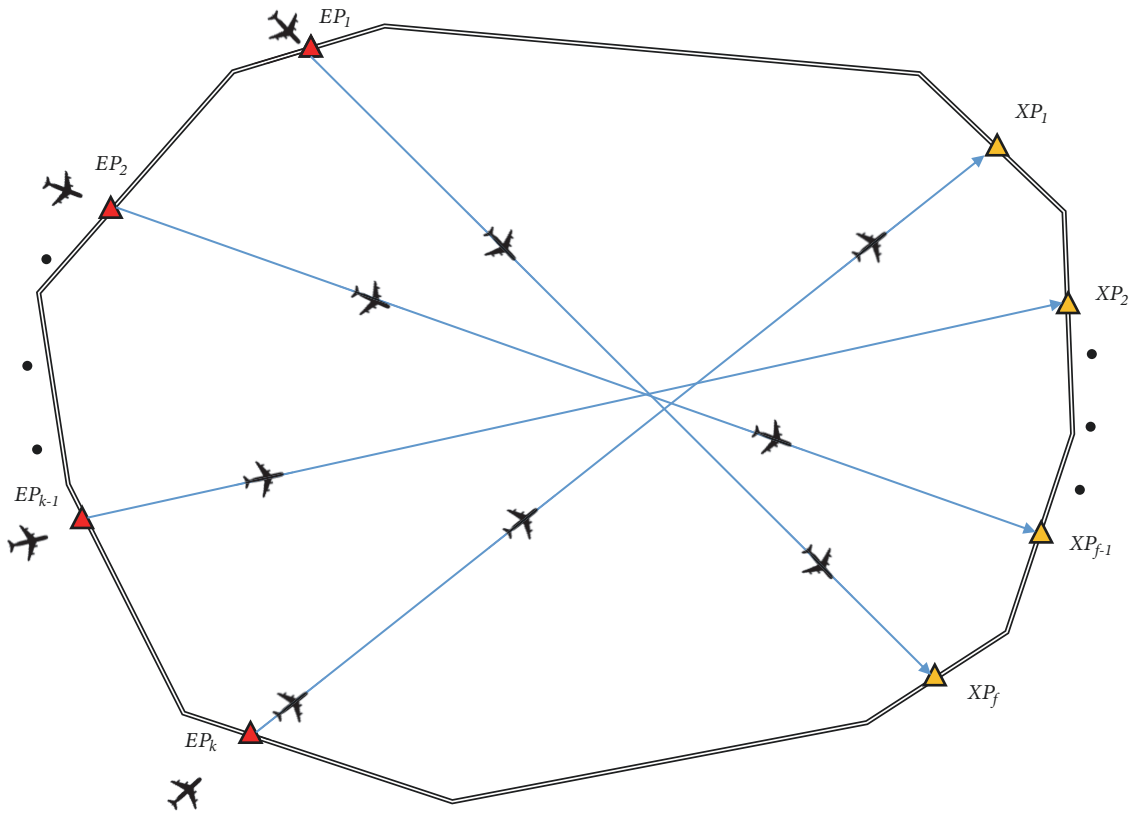

Figure 1: A generic free-route airspace (FRA) configuration.

conflicts prior to entering airspace by assigning them appropriate entry points within the entry areas. The flexible entry point assignment resolves pairwise aircraft conflicts through change of route intersection geometry which alters minimum separation time between aircraft pairs. A suitable entry point assignment combination ensures the reduction of airborne delays required for conflict resolution between aircraft pairs.

Two different types of conflicts can emerge between aircraft during their flight within the described airspace in the horizontal plane: crossing conflicts and trailing conflicts (Figure 3). The crossing conflicts are checked for three different intersection geometries: conflicts in intersecting, converging, and diverging routes (Figures 3(a)–3(c)) to calculate the minimum separation time between aircraft that fly over the same conflict points.

Each conflict point requires a specific time separation between aircraft pairs depending on aircraft speeds and encounter geometry. This time separation is described by [24] as follows.

$$T_{ii'} = \frac{D_{\min}}{V_i V_{i'} \left|\sin\left(\theta_{ii'}\right)\right|} \sqrt{\left(V_i\right)^2 + \left(V_{i'}\right)^2 - 2V_i V_{i'} \cos\left(\theta_{ii'}\right)} \quad (1)$$

In (1), $D_{\min}$ is the minimum separation distance, V_i and $V_{i'}$ are airspeeds of leading and trailing aircraft, respectively, and $\theta_{ii'}$ is the route crossing angle. In order to ensure safe separation between aircraft, one aircraft should be delayed by $T_{ii'}$ prior to airspace entry point (pretactical level). Airspeeds V_i and $V_{i'}$ are assumed to be optimal (best range) airspeeds at the given flight level and they depend on aircraft performance category (APC). In this study, aircraft are classified into three different performance categories: regional jet (RJ), narrow-body jet (NB), and wide-body jet (WB). Trailing conflicts may occur between aircraft flying on the same routes. No overtaking is allowed within the airspace; therefore the separation is maintained by delaying trailing aircraft in pretactical level. Aircraft are assumed to fly with optimal cruise airspeeds at the given flight level.

2.2. Vector Deflection Maneuver. A vector deflection maneuver is proposed to resolve aircraft conflicts in pretactical level (Figure 4). The maneuver consists of two phases: steady coordinated turns and steady straight flights with zero bank angle in the horizontal plane. The vector maneuver uses deflection angle (ψ_i), bank angle (ϕ_i), and maneuver distance (l_i) as decision variables. Other variables such as turning radius (r_i), distance traveled along the arc (a_i), projected arc distance on the undeflected route (b_i), and deflected straight route (l_{di}) are calculated based on these decision variables which are limited in the model with upper and lower values due to operational constraints. Bank angle variations for vectored and nonvectored aircraft are presented in Figure 5.

Aircraft fuel consumption for a given airspeed during the cruise operation depends on distance traveled and propulsive characteristics of aircraft. Turning maneuvers, on the other

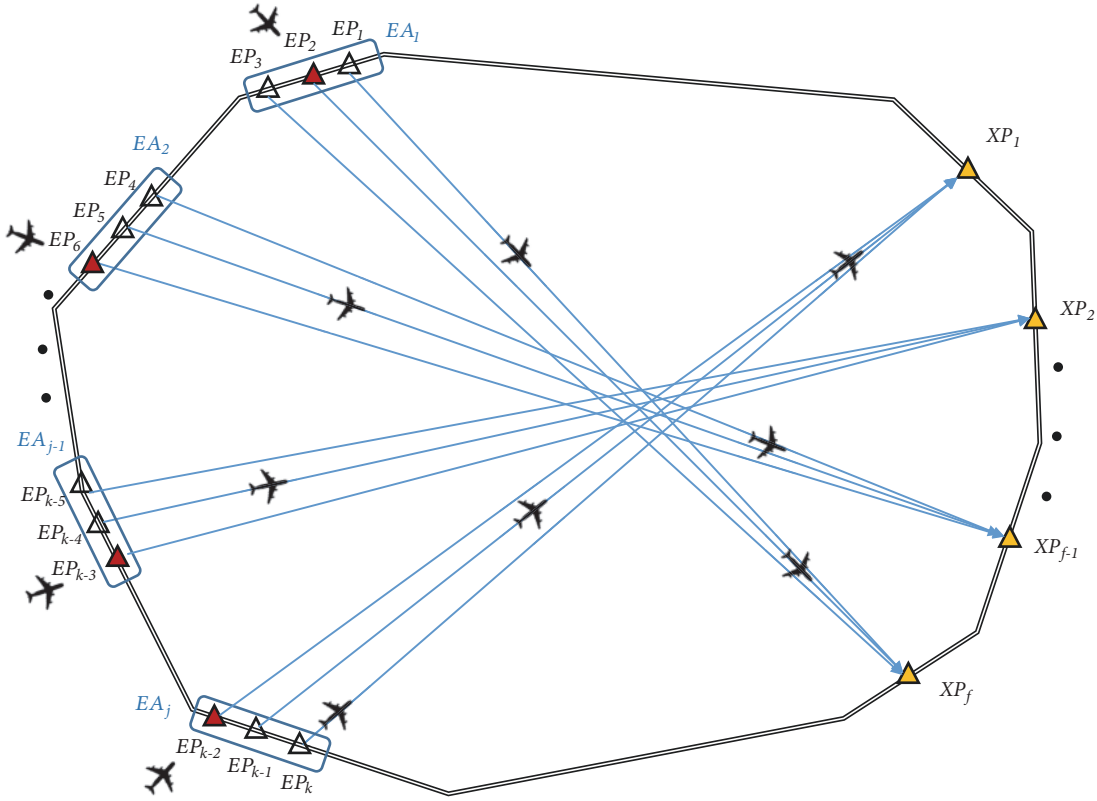

Figure 2: The flexible entry point airspace geometry.

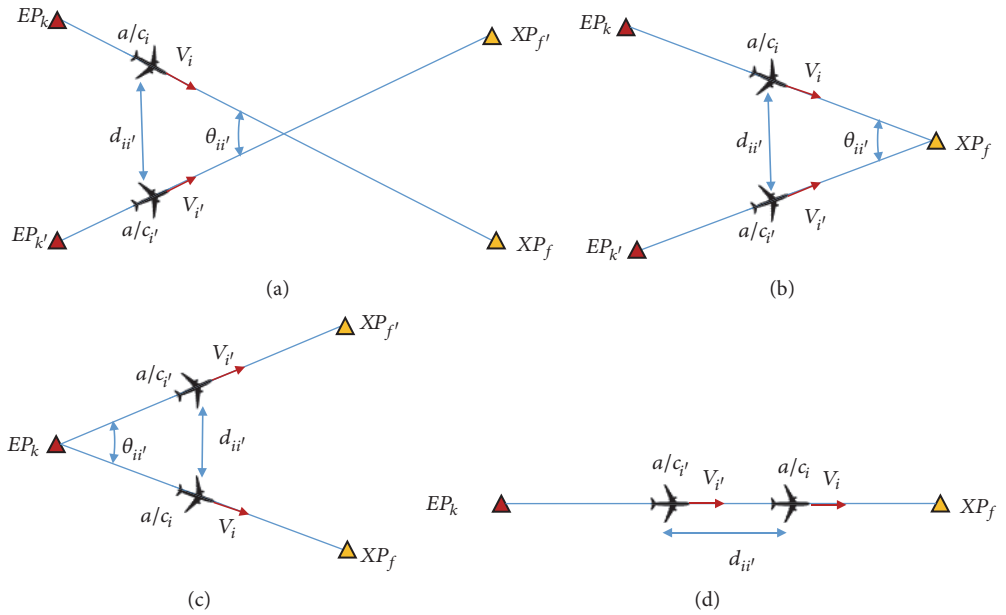

Figure 3: Conflict geometries: crossing conflicts (a) in intersecting routes, (b) converging routes, and (c) diverging routes and (d) trailing conflict in the same route.

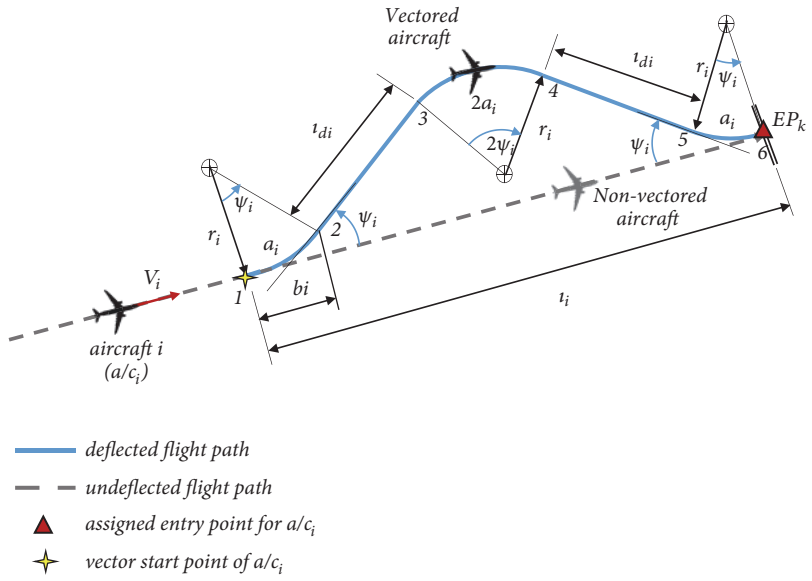

Figure 4: Vector deflection maneuver.

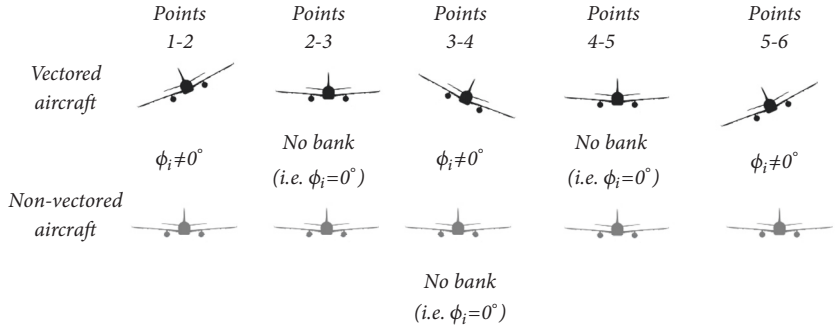

Figure 5: Bank angle variation of vectored and nonvectored aircraft along their flight paths.

hand, create extra fuel burnt not only due to the extended flight path but also due to the increase in the bank angle which results in higher load factors. The proposed model takes bank angle effects into consideration while calculating the fuel consumption. The extra fuel burnt per aircraft along the deflected flight path can be described as follows.

$$w_f = FC_t \bullet 4a_i + FC_{nb} \bullet 2l_{di} - FC_{ud} \bullet l_i \quad (2)$$

While the first two terms in (2) correspond to the amount of fuel burnt along the deflected flight path including total distance traveled along arcs and deflected straight routes, the latter corresponds to the amount of fuel burnt along vector maneuver distance. Therefore, FC_{nb}, and FC_{ud} are fuel consumption rates per unit distance during the straight level flight. For the given aircraft performance category, airspeed, and flight level, these values are constant such that

$$FC_{nb} = FC_{ud} = \chi_{v,o}. \quad (3)$$

FC_t is the fuel consumption rate per unit distance during the coordinated turn and it can be expressed in terms of a third order polynomial of bank angle using curving fitting technique such that

$$FC_t = \chi_{v,o} + \chi_{v,1} \bullet \phi_i + \chi_{v,2} \bullet \phi_i^2 + \chi_{v,3} \bullet \phi_i^3. \quad (4)$$

In (3) and (4), $\chi_{v,o}$, $\chi_{v,1}$, $\chi_{v,2}$, and $\chi_{v,3}$ are regression coefficients found in kg/NM for the performance category v at the given altitude.

3. Mathematical Model

Figure 6 presents the general methodology of the proposed two-step solution approach for minimum airborne delay and extra fuel consumption due to vector deflection maneuvers. In order to evaluate the proposed flexible entry point approach, a baseline case representing fixed entry point FRA is generated as the reference. Estimated time of arrivals (ETA), aircraft performance category (APC), and airspace exit points (XP) of each flight are generated randomly as inputs for both cases. A predefined entry point is provided for each flight in the baseline case while flexible entry point approach assigns each flight to the most suitable entry point within the predefined entry area. In the baseline case, the

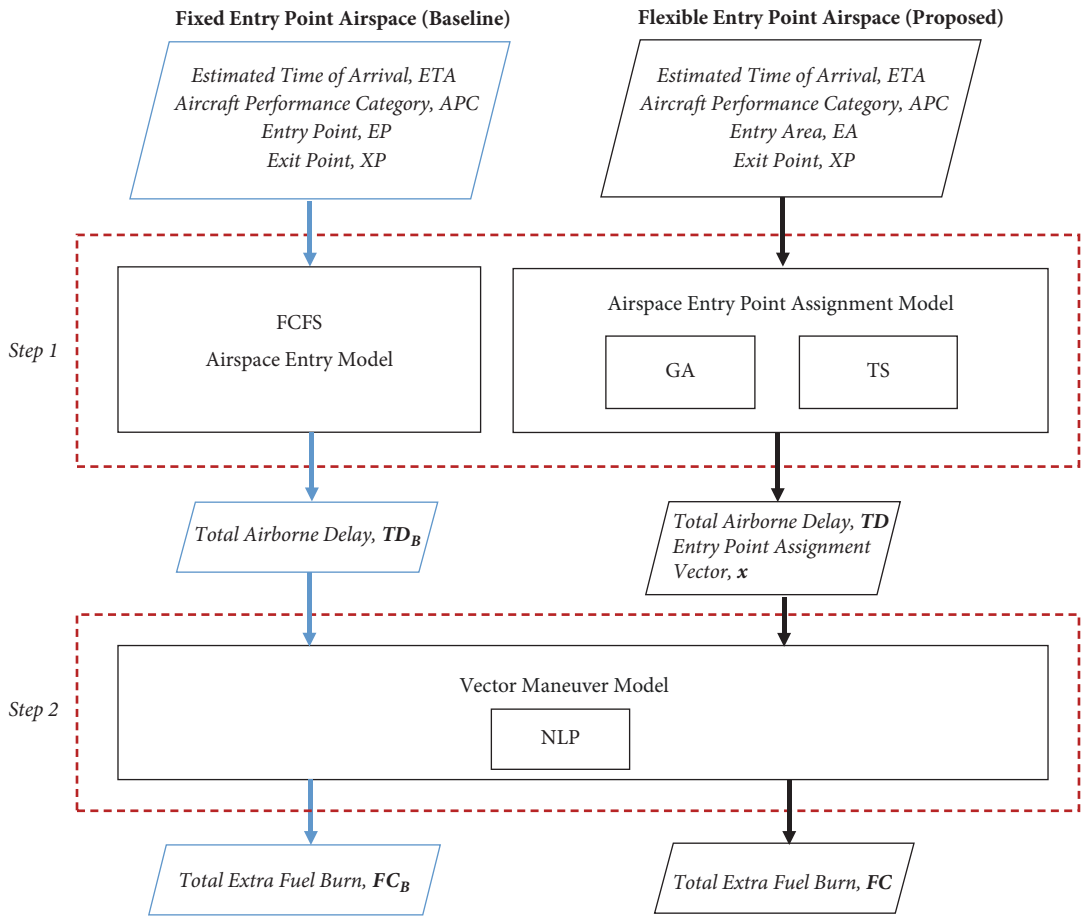

Figure 6: Flow diagram of the two-step model.

total and individual airborne delays are estimated based on first come first served (FCFS) discipline. Flexible entry point assignment also obtains the total and individual airborne delays as well as entry point assignment vector using genetic algorithms (GA) and tabu search (TS) metaheuristics. Upon the estimation of airborne delays, minimum fuel consumption per aircraft is estimated using vector deflection model for both cases.

3.1. First Step: Entry Point Assignment Model. In this section entry point assignment model is presented. The aim is to assign each aircraft to the most suitable entry point according to their entry area to avoid conflict when aircraft is entering into the sector. The main idea of avoiding conflicts is changing conflict geometries just by adjusting entry point. The model seeks for the most appropriate entry point assignment for aircraft, and if it is necessary, the model imposes airborne delay to aircraft. The following assumptions are imposed on the model in addition to the ones described in Section 2.1:

(1) Each aircraft should be assigned to an entry point within its predefined entry area.

(2) Adjacent entry points in the same entry area are located 10 NM apart.

(3) Airspeed and altitude of each aircraft are constant during their flight within the FRA.

Therefore, sets, parameters, variables, objective function, and constraints are given as follows:

Sets

I: Set of aircraft $i, i_1, i_2 \in I$

J: Set of entry areas $j, \in J$

K: Set of entry points $k, k_1, k_2 \in K$

L: Set of exit points $l, l_1, l_2 \in L$

V: Set of aircraft performance category $v, v_1, v_2 \in$

N: Set of intersection points $n, \in N$.

Parameters

M: Big number enough

D_{min}: Minimum separation distance between aircraft

g_i: Scheduled airspace entry time of aircraft i

t_i: Performance category of aircraft i

r_i: Entry area of aircraft i

e_i: Exit point of aircraft i

bg_i: Entry point of aircraft i for baseline scenario

h_v: Airspeed of performance category v

d_{kn}: Distance between entry point k and intersection point n

td_{kl}: Distance between entry point k and exit point l

$sreq_{v_1v_2n}$: Separation time on intersection point n between aircraft performance category v_1 and v_2

$treq_{k_1k_2v_1v_2l}$: Separation time at exit point l between aircraft flying from entry point k_1 and k_2 with performance category v_1 and v_2

$breq_{l_1l_2v_1v_2k}$: Separation time at entry point k between aircraft flying to exit point l_1 and l_2 with performance category v_1 and v_2

u_{jk}: 0-1 parameter that is one if entry point k is in entry area j; otherwise, it is zero

o_{kln}: 0-1 parameter that is one if an aircraft flies from entry point k to exit point l via intersection point n; otherwise, it is zero.

Variables

q_{ik}: Actual entry time of aircraft i at entry point k

w_i: Airborne delay of aircraft i

p_{ikn}: Fly over time of aircraft i from entry point k at intersection point n

c_{ikl}: Fly over time of aircraft i from entry point k at exit point i

$e_{1i_1i_2}$: 0-1 variable that is 1 if aircraft i_2 flies over intersection point before aircraft i_1; otherwise, it is zero

$b_{1i_1i_2}$: 0-1 variable that is 1 if aircraft i_2 enters and leaves the airspace before aircraft i_1; otherwise, it is zero

$b_{2i_1i_2}$: 0-1 variable that is 1 if aircraft i_2 exits the airspace before aircraft i_1; otherwise, it is zero

$b_{3i_1i_2}$: 0-1 variable that is 1 if aircraft i_2 enters the airspace before aircraft i_1; otherwise, it is zero

x_{ik}: 0-1 variable that is 1 if aircraft i is assigned to entry point k; otherwise, it is zero.

The first step of mathematical formulation is as follows.

$$\min \quad \sum_i w_i \tag{5}$$

$$\text{Subject to} \quad \sum_{k|u_{jk}=1} x_{ik} = 1 \quad \forall i, j \mid j = r_i \tag{6}$$

$$\sum_{k|u_{jk}=1,k=bg(i)} x_{ik} = 1 \quad \forall i, j \mid j = r_i \tag{7}$$

$$q_{ik} = g_i + w_i \quad \forall i, k \tag{8}$$

$$p_{ikn} = q_{ik} + \frac{d_{kn}}{h_v} \quad \forall i, k, n, v \mid v = t_i \tag{9}$$

$$c_{ikl} = q_{ik} + \frac{TD_{kl}}{h_v} \quad \forall i, k, l, v \mid v = t_i \tag{10}$$

$$q_{i_2k} - q_{i_1k} \geq \frac{D_{min}}{h_v} - \left(2 - x_{i_1k} - x_{i_2k}\right) \bullet M - b_1\left(i_1, i_2\right) \bullet M \quad \forall i_1, i_2, k, v \mid i_1 \neq i_2,\ v = t_{i_1},\ e_{i_1} = e_{i_2} \tag{11}$$

$$q_{i_1k} - q_{i_2k} \geq \frac{D_{min}}{h_v} - \left(2 - x_{i_1k} - x_{i_2k}\right) \bullet M - b_1\left(1 - i_1, i_2\right) \bullet M \quad \forall i_1, i_2, k, v \mid i_1 \neq i_2,\ v = t_{i_2},\ e_{i_1} = e_{i_2} \tag{12}$$

$$c_{i_2kl} - c_{i_1kl} \geq \frac{D_{min}}{h_v} - \left(2 - x_{i_1k} - x_{i_2k}\right) \bullet M - b_1\left(i_1, i_2\right) \bullet M \quad \forall i_1, i_2, k, v, l \mid i_1 \neq i_2,\ v = t_{i_2},\ e_{i_1} = e_{i_2} \tag{13}$$

$$c_{i_1kl} - c_{i_2kl} \geq \frac{D_{min}}{h_v} - \left(2 - x_{i_1k} - x_{i_2k}\right) \bullet M - b_1\left(1 - i_1, i_2\right) \bullet M \quad \forall i_1, i_2, k, v, l \mid i_1 \neq i_2,\ v = t_{i_1},\ e_{i_1} = e_{i_2} \tag{14}$$

$$q_{i_2k} - q_{i_1k} \geq breq_{l_1l_2v_1v_2k} - \left(2 - x_{i_1k} - x_{i_2k}\right) \bullet M - b_3\left(i_1, i_2\right) \bullet M \quad \forall i_1, i_2, l_1, l_2, k, v_1, v_2 \mid i_1 \neq i_2,\ v_1 = t_{i_1},\ v_2 = t_{i_2},\ e_{i_1} \neq e_{i_2},\ l_1 = e_{i_1},\ l_2 = e_{i_2} \tag{15}$$

$$q_{i_1k} - q_{i_2k} \geq breq_{l_1l_2v_1v_2k} - \left(2 - x_{i_1k} - x_{i_2k}\right) \bullet M - b_3\left(1 - i_1, i_2\right) \bullet M \quad \forall i_1, i_2, l_1, l_2, k, v_1, v_2 \mid i_1 \neq i_2,\ v_1 = t_{i_1},\ v_2 = t_{i_2},\ e_{i_1} \neq e_{i_2},\ l_1 = e_{i_1},\ l_2 = e_{i_2} \tag{16}$$

$$c_{i_2k_2l} - c_{i_1k_1l} \geq treq_{k_1k_2v_1v_2l} - \left(2 - x_{i_1k_1} - x_{i_2k_2}\right) \bullet M - b_2\left(i_1, i_2\right) \bullet M \quad \forall i_1, i_2, k_1, k_2, l, v \mid i_1 \neq i_2,\ v_1 = t_{i_1},\ v_2 = t_{i_2},\ e_{i_1} = e_{i_2},\ k_1 \neq k_2,\ l = e_{i_1} \tag{17}$$

$$c_{i_1k_1l} - c_{i_2k_2l} \geq treq_{k_1k_2v_1v_2l} - \left(2 - x_{i_1k_1} - x_{i_2k_2}\right) \bullet M - b_2\left(1 - i_1, i_2\right) \bullet M \quad \forall i_1, i_2, k_1, k_2, l, v \mid i_1 \neq i_2,\ v_1 = t_{i_1},\ v_2 = t_{i_2},\ e_{i_1} = e_{i_2},\ k_1 \neq k_2,\ l = e_{i_1} \tag{18}$$

$$p_{i_2k_2n} - p_{i_1k_1n} \geq sreq_{v_1v_2n} - \left(2 - x_{i_1k_1} - x_{i_2k_2}\right) \bullet M - e_1\left(i_1, i_2\right) \bullet M \quad \forall i_1, i_2, l_1, l_2, k_1, k_2, v_1, v_2 \mid i_1 \neq i_2,\ v_1 = t_{i_1},\ v_2 = t_{i_2},\ e_{i_1} \neq e_{i_2},\ k_1 \neq k_2,\ l_1 = e_{i_1},\ l_2 = e_{i_2},\ o_{k_1l_1n} = 1,\ o_{k_2l_2n} = 1 \tag{19}$$

$$p_{i_1k_1n} - p_{i_2k_2n} \geq sreq_{v_1v_2n} - \left(2 - x_{i_1k_1} - x_{i_2k_2}\right) \bullet M - e_1\left(1 - i_1, i_2\right) \bullet M \quad \forall i_1, i_2, l_1, l_2, k_1, k_2, v_1, v_2 \mid i_1 \neq i_2,\ v_1 = t_{i_1},\ v_2 = t_{i_2},\ e_{i_1} \neq e_{i_2},\ k_1 \neq k_2,\ l_1 = e_{i_1},\ l_2 = e_{i_2},\ o_{k_1l_1n} = 1,\ o_{k_2l_2n} = 1 \tag{20}$$

The objective function (5) of the model is to minimize the total airborne delay. Constraint set (6) ensures that every aircraft is assigned to one entry point which belongs to its entry area. Constraint set (7) ensures that every aircraft is assigned to its own baseline entry point. Constraint sets (8), (9), and (10) calculate the flyover time at the entry point, intersection point, and exit point of the airspace, respectively. Constraint sets (11), (12), (13), and (14) maintain the required separation time between all aircraft pairs for trailing conflicts. Constraint sets (15) and (16) maintain the required separation time between all aircraft pairs for conflicts in diverging routes. Constraint sets (17) and (18) maintain the required separation time for all conflicts in converging routes. Constraint sets (19) and (20) maintain the required separation time between all aircraft pairs for conflicts in intersecting routes. Therefore all possible conflicts between all aircraft pair combinations within the airspace are controlled by the model using the provided constraints.

3.2. Second Step: Vector Deflection Model. Although the first step calculates the minimum airborne delay to resolve conflicts, it does not specify which maneuver to be implemented to aircraft in order to avoid conflicts. The entry point assignment is capable of resolving many potential conflicts without requiring extra resolution maneuvers. In case of a necessity of an airborne delay, the proposed vector deflection model in Section 2.2 can be applied to aircraft prior to their entrance to the airspace. Certainly, there are infinitely many vector deflection maneuvers which can resolve the conflict for the given airborne delay. In this step, the model searches vector deflection resolutions with minimum fuel consumption per aircraft under given constraints as described in Section 2.2. The following assumptions are imposed on the model in addition to the ones described in Section 2.2:

(1) Weight of all aircraft is constant during their vector deflection maneuver.

(2) Airspeed and altitude of each aircraft are constant during the vector deflection maneuver.

(3) Bank angle changes are done instantly during the coordinated turning maneuvers.

(4) Standard atmospheric conditions are valid.

(5) Wind speed and acceleration are zero.

The second step of mathematical formulation is as follows.

Sets

I: Set of aircraft $i, \in I$

V: Set of aircraft performance category $v, \in V$.

Parameters

g: gravitational acceleration

t_i: Performance category of aircraft i

dx_i: Extra distance flown due to airborne delay i

h_V: Airspeed of performance category v

$\chi_{v,o}$: Fuel consumption coefficient with no bank angle for aircraft performance category v

$\chi_{v,1}$: Fuel consumption coefficient with first order bank angle for aircraft performance category v

$\chi_{v,2}$: Fuel consumption coefficient with second order bank angle for aircraft performance category v

$\chi_{v,3}$: Fuel consumption coefficient with third order bank angle for aircraft performance category v.

Variables

R_i: Turn radius of aircraft i

ψ_i: Deflection angle of aircraft i

ϕ_i: Bank angle of aircraft i

l_i: Maneuver distance of aircraft i

a_i: Arc distance traveled by aircraft i during turning maneuver

b_i: Total distance traveled by aircraft i projected on the undeflected route during turning maneuver

l_{di}: Distance traveled by aircraft i along the deflected route with no bank

f_{1_i}: Fuel consumption of aircraft i during turning maneuver

Table 1: Cruise airspeed and fuel consumption rates of aircraft performance categories at 33000 feet.

Aircraft Performance Category	Airspeed, h_v (knots)	Fuel Consumption Regression Coefficients (kg/NM)			
		$\chi_{v,o}$	$\chi_{v,1}$	$\chi_{v,2}$	$\chi_{v,3}$
Regional jet, RJ (v=1)	388	1.284	0.9147	0.05794	4.243
Narrow-body jet, NB (v=2)	426	1.371	0.9771	0.06189	5.282
Wide-body jet, WB (v=3)	482	6.416	4.572	0.2896	17.09

f_{2_i}: Fuel consumption of aircraft i along the deflected route with no bank

f_{3_i}: Fuel consumption of aircraft i along the undeflected route.

Objective

$$\min \quad \sum_i FC_{t_i} \bullet 4a_i + FC_{nb_i} \bullet 2l_{di} - FC_{ud_i} \bullet l_i \tag{21}$$

$$\text{Subject to} \quad r_i = \frac{{h_v}^2}{g \bullet \tan(\phi_i)} \quad \forall i, v \mid v = t_i \tag{22}$$

$$a_i = r_i \psi_i \quad \forall i \tag{23}$$

$$l_{di} = \frac{l_i - b_i}{2 \bullet \cos(\psi_i)} \quad \forall i \tag{24}$$

$$b_i = \bullet r_i \bullet \sin(\psi_i) \quad \forall i \tag{25}$$

$$4a_i + 2l_{di} - l_i - dx_i = 0 \quad \forall i \tag{26}$$

$$4b_i \le l_i \quad \forall i \tag{27}$$

$$FC_{t_i} = \left(\chi_{v,o} + \chi_{v,1} \bullet \phi_i + \chi_{v,2} \bullet {\phi_i}^2 + \chi_{v,3} \bullet {\phi_i}^3\right) \quad \forall i, v \mid v = t_i \tag{28}$$

$$FC_{nb_i} = (\chi_{v,o}) \quad \forall i, v \mid v = t_i \tag{29}$$

$$FC_{ud_i} = (\chi_{v,o}) \quad \forall i, v \mid v = t_i \tag{30}$$

$$0 \le \psi_i \le \frac{\pi}{2} \quad \forall i \tag{31}$$

$$0 \le \phi_i \le \frac{\pi}{6} \quad \forall i \tag{32}$$

$$0 \le l_i \le 40 \quad \forall i \tag{33}$$

The objective function of the second model (21) is to minimize total extra fuel consumption. Constraint set (22) calculates the turn radius for each aircraft. Constraint sets (23)-(25) calculate the distance traveled along the arc (a_i), deflected straight route (l_{di}), and projected arc distance (b_i) on the undeflected route, respectively. Constraint set (26) guarantees that the distance traveled during vector deflection maneuver satisfies the required airborne delay. Constraint set (27) ensures that the sum of arc distances projected on undeflected route cannot be longer than vector maneuver distance. While constraint set (28) estimates fuel consumption rates per unit distance during the coordinated turns, constraint sets (29)-(30) provide fuel consumption rates per unit distance during straight level flights along deflected and undeflected flight paths. Table 1 presents the cruise airspeed and fuel consumption rates per unit distance estimated based on the values provided in BADA [25] for each aircraft performance category at 33000 feet (FL330).

4. Metaheuristic Algorithms

Metaheuristic algorithms are an effective way of using trial and error methods to produce acceptable solutions to a complex problem. The complexity of the problems makes it difficult to evaluate all possible solutions. These algorithms aim to obtain good solution within an acceptable period of time, but they do not guarantee achieving the global optimum result. In this study, genetic algorithms and tabu search are proposed to solve the mathematical model presented in the first step.

4.1. The Proposed Genetic Algorithm. The entry point assignment model is a complex model so it is difficult to solve this problem by MIP solver within the reasonable time period. Thus, we present a genetic algorithm to deal with this problem. Genetic algorithms (GA) are search algorithms based on Darwin's theory of evolution and described by John Holland [26]. Genetic algorithms try to achieve the best solution by imitating natural selection. In genetic algorithms, each chromosome represents a solution and multiple chromosomes come together to form a population. Chromosomes pass their selection, crossing, and mutation steps to transfer their genes to the next generation. Highly compatible chromosomes are more likely to transfer genes to subsequent generations.

4.1.1. Chromosomes Structure and Initial Population. Chromosomes come from genes, and each gene refers to entry point for each aircraft. An example of chromosomes structure for six aircraft and twelve entry points can be seen in Table 2. Each gene belongs to only one aircraft and each aircraft is assigned to one entry point according to its entry area. During the process of obtaining initial population, each aircraft is assigned to an entry point randomly according to its entry area; therefore, infeasible gene structures can be prevented.

4.1.2. Fitness Function. According to entry point assignment, fitness function of all chromosomes is calculated. The algorithm checks for any conflicts between each aircraft pair. If

Table 2: Chromosomes structure.

Aircraft 1	Aircraft 2	Aircraft 3	Aircraft 4	Aircraft 5	Aircraft 6
EP11	EP 7	EP 4	EP 2	EP 9	EP 6

Parent1	Aircraft 1	Aircraft 2	Aircraft 3	Aircraft 4	Aircraft 5	Aircraft 6
	EP11	EP 7	EP 4	EP 2	EP 9	EP 6
Random Value	0.3	0.6	0.1	0.7	0.9	0.45
Parent2	Aircraft 1	Aircraft 2	Aircraft 3	Aircraft 4	Aircraft 5	Aircraft 6
	EP12	EP 5	EP 6	EP 1	EP 10	EP 4

Offspring 1	Aircraft 1	Aircraft 2	Aircraft 3	Aircraft 4	Aircraft 5	Aircraft 6
	EP11	EP 5	EP 4	EP 1	EP 10	EP 6
Offspring 2	Aircraft 1	Aircraft 2	Aircraft 3	Aircraft 4	Aircraft 5	Aircraft 6
	EP12	EP 7	EP 6	EP 2	EP 9	EP 4

Figure 7: An example of uniform crossover operator.

there is a conflict, the algorithm randomly decides which aircraft should be delayed. For this process, genetic algorithm generates a random number ranging from 0 to 1 for both aircraft, and the aircraft having the lower value is imposed to delay. This method allows different solutions in the search space to be reached. Finally, the total airborne delay of each chromosome is calculated.

4.1.3. Selection Process and Elitism. The selection process is a critical step to determine population diversity and selection bias that affect performance of GA significantly. If the selection pressure increases, the population diversity decreases. In the opposite case, if diversity increases in the population, good solutions are beginning to decrease. Keeping these two factors in balance is an important step for GA's success [27]. In this study, the selection is performed using the roulette wheel method that allows chromosomes with good adaptability to transmit more genes to the next generation. Elitism is used to reduce genetic drift by copying the best chromosomes into future generations in the final step.

4.1.4. Crossover. The crossover operator allows for the generation of new individuals as a result of mutual exchange of the genes of the chromosomes which will be crossed after the selection. With this method, some features of previous generations can be transferred to the new generation. The success of the crossover process depends on the proper coding of the chromosomes according to the probing. In this study, new chromosomes are produced through the use of reciprocal displacement of genes belonging to the same aircraft between selected chromosome pairs. This process is included in the literature as uniform crossover (Figure 7). In the crossover process, a value between 0 and 1 is produced randomly for each pair of genes, and if this value is greater than 0.5, the displacement takes place between the gene pairs.

4.1.5. Mutation and Elitism. The mutation operator modifies one or more gene values randomly to increase the diversity of the solution. Furthermore, the mutation operator enables genetic algorithms to converge a feasible solution more rapidly. As a result of the mutation process, a new chromosome structure is obtained by replacing the selected genes with another entry point in its entry region (Figure 8).

4.2. The Proposed Tabu Search. The tabu search (TS) algorithm was developed by Glover in 1986 [28]. The TS algorithm is an intuitive method that finds the best value by moving away from the local optimum. TS algorithm, which can be used to solve many different problems, has a flexible structure to produce the best or nearest solutions. By using the memory structure, some solutions are banned from being produced over a certain number of iterations. These solutions are added to tabu list and called "tabu". The primary task of tabu list is to ensure that the algorithm achieves the overall best value by avoiding local best values. In some cases, if a tabu move solution gives a better solution than the best found so far, this solution is no longer classified as tabu. By this way, the TS algorithm helps to improve the harmonization value by using aspiration criterion.

4.2.1. Initial Solution. The TS algorithm first needs an initial solution to start searching for a solution. Generating a good initial solution significantly improves the success of the algorithm. In this study, baseline airspace entry points are chosen as the initial solution (Table 3).

4.2.2. Neighborhood Structure. Generating neighborhood solutions helps to improve the existing solution by changing airspace entry points randomly within the entry area for selected aircraft. Generation process is shown in Table 4.

Individual	Aircraft 1	Aircraft 2	Aircraft 3	Aircraft 4	Aircraft 5	Aircraft 6
	EP11	EP 7	EP 4	EP 2	EP 9	EP 6
Offspring	Aircraft 1	Aircraft 2	Aircraft 3	Aircraft 4	Aircraft 5	Aircraft 6
	EP11	EP 8	EP 4	EP 2	EP 9	EP 6

Figure 8: An example of mutation operator.

Table 3: Initial solution representation.

Aircraft 1	Aircraft 2	Aircraft 3	Aircraft 4	Aircraft 5	Aircraft 6
EP11	EP 5	EP 5	EP 2	EP 8	EP 11

Table 4: Generating neighborhood.

Existing Solution	Aircraft 1	Aircraft 2	Aircraft 3	Aircraft 4	Aircraft 5	Aircraft 6
	EP11	EP 8	EP 5	EP 2	EP 8	EP 5
Neighborhood Solution 1	Aircraft 1	Aircraft 2	Aircraft 3	Aircraft 4	Aircraft 5	Aircraft 6
	EP11	EP 7	EP 5	EP 2	EP 8	EP 5
Neighborhood Solution 2	Aircraft 1	Aircraft 2	Aircraft 3	Aircraft 4	Aircraft 5	Aircraft 6
	EP11	EP 8	EP 5	EP 3	EP 8	EP 4

Table 5: Tabu list demonstration.

Aircraft	Entry Points											
	1	2	3	4	5	6	7	8	9	10	11	12
1	0	0	0	0	0	0	0	0	0	0	2	0
2	0	0	0	0	0	0	3	0	0	0	0	0
3	0	0	0	0	0	0	0	0	0	0	0	0
4	0	0	0	0	0	0	0	0	0	0	0	0
5	0	0	0	0	0	0	1	0	0	0	0	0
6	0	0	0	0	0	0	0	0	0	0	0	0

Table 4 shows how we obtain two neighborhood solutions. To achieve this process, the second and fourth aircraft are randomly selected, and two different neighbor solutions are produced in addition to the existing solution. In the first neighboring solution, the entry point of the second aircraft is changed randomly while the entry point of the fourth aircraft remains the same. Similarly, in the second neighboring solution, the entry point of the fourth aircraft is changed randomly while the entry point of the second aircraft remains the same in the second neighboring solution.

4.2.3. Short-Term Memory. Tabu list allows the search for the different points in the solution space by banning searched solutions for a certain number of iterations. The number of iterations specifies the length of the tabu list. Tabu list does not interfere to produce neighborhood solution production. However, after the fitness values are calculated, the solutions on the tabu list are called tabu and removed from neighboring solutions. This process is performed using short-term memory [28]. Both the aspiration criterion and the short-term memory structure are used in this study. Tabu list demonstration is shown in Table 5.

In Table 5, tabu length size is chosen as three. To explain the use of tabu list, an example of tabu list structure is given. The entry point 7 for the second aircraft will be kept on the tabu list for three iterations. It is also forbidden to assign the first aircraft on the list to the entry point 11 and the fifth aircraft to the entry point 7. The number of entry points kept on the list varies according to the length of the tabu list.

5. Computational Results

The proposed GA and TS metaheuristics are developed to solve more complex airspace structures of which GAMS/CPLEX solver cannot reach a solution within reasonable time period. A set of small-sized test problems are generated in order to evaluate these metaheuristics. For all test problems, total airborne delays are calculated using GAMS/CPLEX solver, GA, and TS algorithm. The selected parameters of metaheuristics are presented in Table 6. These parameters are determined experimentally. The solution time of the all approaches is set to 900 seconds in order to provide a feasible solution in pretactical time window. A computer with 2.3 GHz Intel Core i7 processor and 16 GB RAM is used in all computations.

Thirty test problems are generated for 180 nm^2 en-route airspace (as presented in Figure 2) at FL330 with three

Table 6: The parameters of metaheuristics.

Genetic Algorithm		Tabu Search Algorithm	
Population Size	50	Neighborhood Solution Size	9
Selection Process	Roulette		
Crossover Rate	0.8	Tabu List Size	7
Mutation Rate	0.1		
Number of Generation	200	Number of Generation	1110

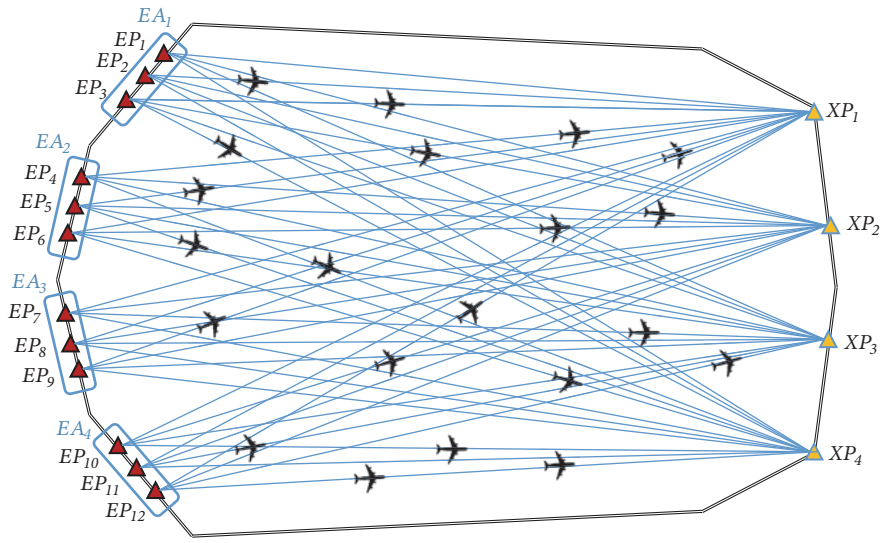

Figure 9: Complex airspace structure.

combinations of 12 routes between four entry areas with 3 entry points and 4 exit points. The numbers of the intersection points for these airspace configurations (i.e., I, II, and III) are 27, 36, and 45, respectively. Hourly traffic flow entering to the airspace is set to 20 aircraft in three different performance categories: regional jets, narrow-body aircraft, and wide-body aircraft. Estimated times of arrival (ETA) based on exponential distribution, aircraft performance categories (APC), entry areas (EA), and exit points (XP) are generated as input parameters using MATLAB. Entry points for the baseline scenario are chosen as the mid-points of each entry area (i.e., EP_2 for EA_1, EP_5 for EA_2, EP_8 for EA_3, and EP_{11} for EA_4). The results of GAMS/CPLEX, GA, and TS are presented for 30 test problems in Table 7. While GAMS/CPLEX results include the values of objective function (z) and CPU time, GA and TS results contain the average and minimum objective function values of three runs for each test problem as well as their average CPU times. The minimum airborne delays found using GA and TS are equal to those of GAMS/CPLEX solver solutions for each test problem. These results demonstrate that the proposed metaheuristics can achieve optimal solutions of GAMS/CPLEX for all test problems.

The complex route network for the generic airspace includes all possible 48 route combinations between the existing entry and exit points (Figure 9). The length of each route is shown in Table 8. In order to test this complex network, two different traffic flow rates are selected as 20 and 25 aircraft per hour. For each traffic flow rate thirty different scenarios are generated.

5.1. Results of Flexible Entry Point Assignment Model. Table 9 provides a comparison of the results found for baseline case of fixed entry points and flexible entry point approach for all scenarios. While baseline results include the values of objective function (z) calculated via using FCFS model in MATLAB, flexible entry point results present the total airborne delays found by using GA and TS as the minimum of three separate runs.

No airborne delays occur in three scenarios (i.e., 6, 20, and 30) with the traffic flow of 20 aircraft per hour for the baseline case. While GA and TS find the same values in 25 scenarios for this traffic flow rate, GA achieved slightly better values than TS in two scenarios (i.e., 14 and 25). When the traffic flow rate is increased to 25 aircraft per hour, GA and TS find the same total airborne delay in 23 scenarios. GA provides better solutions in the remaining scenarios. The average results are demonstrated in Figure 10.

Figure 10 shows that the baseline average delay time for 20 aircraft decreases from 127.2 seconds to 8.4 seconds for GA and 8.6 seconds for TS. The percentages of recovery for GA and TS are 93.4% and 93.3%, respectively. For the 25 aircraft, the average delay in the baseline case is reduced from 193.1 seconds to 21.4 seconds for GA and to 23.2 seconds for TS. The recovery percentages for GA and TS are 88.9% and 88%, respectively. Both algorithms have yielded successful results.

Table 7: Test problem results using GAMS/CPLEX, GA, and TS.

Test Problems	GAMS/CPLEX		TS			GA		
	Z (sec.)	t(sec.)	z_{ave}*(sec.)	z_{min} (sec.)	T_{avg}(sec.)	z_{ave}(sec.)	z_{min}(sec.)	T_{avg}(sec.)
1	**0**	111	0.0	**0**	2.8	0.0	**0**	0.7
2	**0**	112	0.0	**0**	0.3	0.0	**0**	0.7
3	**0**	109	0.0	**0**	6.0	0.0	**0**	2.1
4	**2**	110	2.0	**2**	67.7	2.0	**2**	108.6
5	**0**	113	0.0	**0**	18.4	1.7	**0**	41.9
6	**18**	114	18.0	**18**	67.5	18.0	**18**	112.6
7	**0**	113	0.0	**0**	4.4	0.0	**0**	1.0
8	**0**	114	0.0	**0**	0.4	0.0	**0**	0.8
9	**34**	113	55.0	**34**	73.2	34.0	**34**	124.3
10	**22**	114	22.7	**22**	75.8	24.7	**22**	122.5
11	**0**	144	0.3	**0**	40.8	0.0	**0**	3.8
12	**0**	151	0.0	**0**	2.8	0.0	**0**	1.8
13	**0**	149	0.0	**0**	4.0	0.0	**0**	3.1
14	**0**	150	0.0	**0**	2.3	0.0	**0**	1.3
15	**24**	148	24.0	**24**	94.7	26.0	**24**	154.1
16	**10**	148	10.7	**10**	88.6	10.0	**10**	148.9
17	**4**	149	4.0	**4**	82.4	6.7	**4**	131.8
18	**5**	150	7.7	**5**	95.5	7.3	**5**	153.4
19	**10**	148	13.3	**10**	114.1	23.3	**10**	180.2
20	**3**	152	3.0	**3**	97.7	6.0	**3**	148.4
21	**0**	190	0.0	**0**	20.1	0.0	**0**	8.3
22	**17**	187	17.0	**17**	109.4	17.0	**17**	192.0
23	**0**	188	1.3	**0**	66.2	0.0	**0**	25.0
24	**0**	191	0.0	**0**	4.6	0.0	**0**	1.2
25	**38**	190	38.0	**38**	92.2	38.0	**38**	165.9
26	**1**	191	1.0	**1**	108.6	1.0	**1**	187.0
27	**0**	189	0.0	**0**	1.0	0.0	**0**	1.0
28	**0**	186	0.0	**0**	1.4	0.0	**0**	1.0
29	**12**	190	12.0	**12**	103.7	12.0	**12**	183.9
30	**10**	187	10.0	**10**	102.8	10.0	**10**	174.8

Table 8: Routes distances in complex airspace.

Entry Points	Route Distances (nm)			
	XP1	XP2	XP3	XP4
1	180.0	189.7	216.3	247.5
2	180.2	186.8	210.9	240.8
3	181.1	184.3	205.9	234.3
4	186.8	180.2	193.1	216.3
5	189.7	180.0	189.7	210.9
6	193.1	180.2	186.8	205.9
7	205.9	184.3	181.1	193.1
8	210.9	186.8	180.2	189.7
9	216.3	189.7	180.0	186.8
10	234.3	201.2	182.4	181.1
11	240.8	205.9	184.3	180.2
12	247.5	210.9	186.8	180.0

Table 9: The airborne delays (sec.) and CPU times (sec.) of the all scenarios with 20 and 25 aircraft per hour.

Scenario Number	20 Aircraft					25 Aircraft				
	Baseline	GA	t_{ort}	TS	t_{ort}	Baseline	GA	t_{ort}	TS	t_{ort}
1	94	0	14.7	0	22.0	242	26	252.4	26	254.6
2	284	3	173.8	3	171.6	195	17	231.6	17	246.0
3	271	1	173.5	1	157.0	13	0	5.7	0	4.1
4	86	0	4.4	0	21.8	412	61	325.9	84	337.4
5	36	0	10.9	0	19.1	18	0	5.1	0	5.6
6	0	0	4.3	0	0.5	91	27	254.7	27	258.8
7	29	0	4.5	0	5.1	305	21	244.9	21	251.9
8	352	36	158.3	36	163.5	247	28	283.6	28	280.4
9	41	0	5.9	0	5.1	122	11	228.3	11	223.6
10	59	0	4.4	0	10.7	7	0	5.6	0	3.3
11	39	0	4.4	0	5.6	162	0	8.7	0	50.1
12	65	14	171.5	14	159.4	180	23	276.6	23	274.3
13	291	32	172.2	32	175.0	110	25	236.9	25	224.0
14	265	21	161.4	22	166.4	512	121	372.4	129	347.4
15	312	2	175.9	2	170.4	206	34	316.7	34	314.8
16	46	0	6.9	0	11.2	221	23	240.6	23	252.6
17	81	0	4.4	0	3.7	319	62	301.5	70	305.5
18	301	20	148.3	20	141.3	83	0	6.3	0	42.8
19	61	18	149.0	18	149.7	266	27	327.3	33	325.7
20	0	0	4.6	0	0.5	419	0	33.7	6	267.9
21	230	35	181.0	35	164.3	119	0	7.9	0	74.0
22	61	0	5.7	0	6.8	143	25	219.1	25	212.2
23	5	0	5.6	0	4.6	32	0	12.5	0	17.4
24	26	0	5.8	0	2.2	194	0	11.8	0	26.4
25	289	38	171.7	43	149.1	94	12	258.4	14	258.7
26	49	5	180.9	5	155.7	146	0	6.2	0	15.3
27	141	20	168.7	20	162.1	498	48	335.2	50	307.6
28	113	4	137.5	4	130.4	278	50	287.8	50	272.1
29	189	2	157.9	2	160.9	3	0	5.9	0	2.8
30	0	0	4.5	0	0.5	157	0	19.0	0	35.4

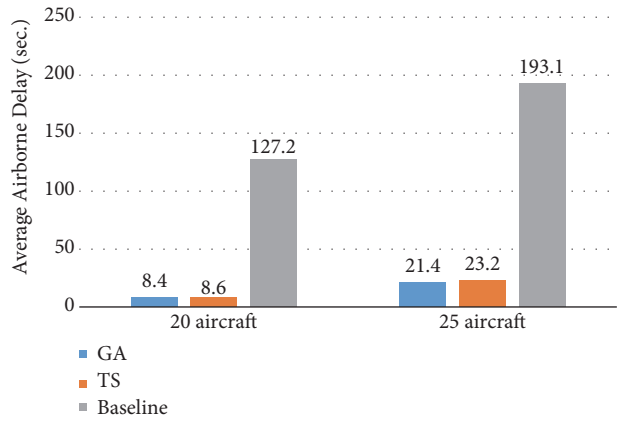

Figure 10: The average airborne delay for two different aircraft flow rates.

The results show that airborne delays due to conflicts can be reduced significantly using flexible entry point assignment.

5.2. Results of Vector Deflection Model. Table 10 presents the total fuel consumption for each scenario due to vector maneuvers based on the total airborne delay calculated in the first step of the model. Similar to Table 9, the baseline case represents the results found for fixed entry point configuration based on FCFS discipline, while GA and TS columns provide the results of flexible entry point approach for all scenarios calculated in GAMS/CONOPT solver and each scenario is estimated in less than 10 seconds.

The fuel consumption results based on GA and TS airborne delays are the same or very close to each other in all scenarios for the traffic flow rate of 20 aircraft per hour. GA-based results, on the other hand, are better than TS-based results in five scenarios and worse than TS-based results in one scenario. The fuel consumption averages are presented in Figure 11.

Aircraft vector deflection model is implemented in both baseline and metaheuristics-based airborne delays. The baseline, GA-based, and TS-based fuel consumption averages are found to be 201.4, 9.3, and 9.4 kg, respectively for 20 aircraft

Table 10: The delayed aircraft vector deflection model fuel consumption (kg).

Scenario Number	20 Aircraft			25 Aircraft		
	Baseline	GA-based	TS-based	Baseline	GA-based	TS-based
1	182.28	0	0	439.03	11.9	11.9
2	638.64	1.9	1.9	354.47	10.7	10.7
3	170.69	0.6	0.6	8.23	0	0
4	53.12	0	0	384.05	91	105.5
5	16.78	0	0	11.41	0	0
6	0	0	0	152.33	17	17
7	18.3	0	0	452.02	24.6	24.6
8	403.88	83.6	83.6	211.66	31.4	31.4
9	95.19	0	0	127.42	5.4	5.4
10	64.43	0	0	16.42	0	0
11	90.57	0	0	331.98	0	0
12	103.62	20.9	20.9	170.02	12.58	12.58
13	473.5	20.1	20.1	197.55	15.7	15.7
14	498.86	15.2	15.3	699.73	138	158.9
15	568.93	7.1	7.1	235.45	50.4	50.4
16	106.74	0	0	439.81	14.5	14.5
17	50.96	0	0	430.29	32.4	35.8
18	618.74	12.6	12.6	86.38	0	0
19	39.42	8.3	8.3	367.17	40.9	55.01
20	0	0	0	270.53	0	0
21	444.4	25.2	25.2	260.96	0	0
22	141.64	0	0	198.04	15.7	15.7
23	11.76	0	0	74.39	0	0
24	60.5	0	0	398.77	0	0
25	276.37	47.9	49.3	105.24	16.2	8.8
26	66.59	12.5	12.5	188.11	0	0
27	146.51	9.3	9.3	564.78	89.8	94.4
28	261.83	9.4	9.4	600.61	115.6	115.6
29	437.79	4.7	4.7	7.09	0	0
30	0	0	0	249.33	0	0

per hour, while for the 25 aircraft, the baseline, GA-based, and TS-based fuel consumption averages are found to be 267.7, 24.5, and 26.1 kg, respectively. The flexible entry point assignment obtained from GA and TS reduces the extra fuel consumption considerably. This is mainly because this approach resolves most of the possible conflicts via switching the entry points rather than implementing vector maneuvers. Therefore, both the number of aircraft conflicts and the required average airborne delays for conflict resolution are reduced significantly. The vector maneuvers are only implemented to fewer number of aircraft than those of the baseline scenarios. Reduced airborne delay leads to less extra fuel consumption caused by vector maneuvers.

6. Conclusion

The proposed two-step approach provided aircraft conflict resolutions with minimum airborne delay through flexible entry point assignment using GA and TS metaheuristics and offered vector deflection maneuvers with minimum extra fuel consumption for delayed aircraft within FRA using NLP. The optimal solutions in both steps are obtained in reasonable times for a wide range of scenarios including test problems and more complex and realistic airspace routes structures. The proposed approach can be a good candidate for a decision-support system for effective conflict management in pretactical level. Through the entry point assignment and vector resolution advisories, air traffic controller's occupancy time can be reduced dramatically. It increases the airspace capacity through the reduction of airborne delays as well. The economic and environmental efficiency of the flight operations can be further enhanced through reduction of extra fuel consumption. The proposed vector deflection model also enables air traffic controller to choose limit values of maneuvering distance, bank angle, and deflection angle constraints. In future studies, the problem can be formulated as a multiobjective mathematical model that aims to find optimal airborne delay and fuel consumption simultaneously. Aircraft conflict resolution can also be extended to airspeed and altitude change maneuvers and, therefore, the model can

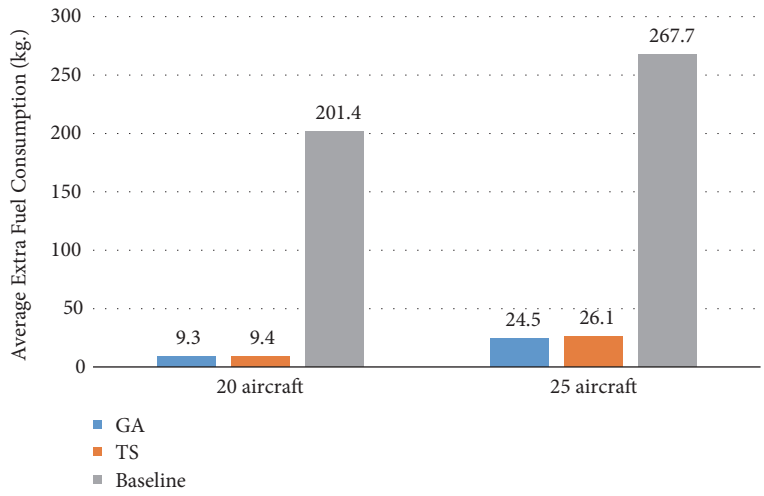

Figure 11: The average extra fuel consumption rates.

be applied to terminal airspaces. Inclusion of uncertainties such as wind variations in this approach can be a useful extension for tactical CD&R at low level en-route and terminal airspaces.

Data Availability

The aircraft input parameters (ETA, APC, EA, EP, and XP) are randomly generated in MATLAB, and the data used to support the findings of this study are available from the corresponding author upon request.

Conflicts of Interest

The authors declare that there are no conflicts of interest regarding the publication of this paper.

Acknowledgments

This study was supported by Anadolu University Scientific Research Projects Commission under grant number 1707F454.

References

[1] "Aviation. benefits beyond borders report," Tech. Rep., Air Transport Action Group, 2018.

[2] Airbus Group, "Global market forecast 2017/2036, growing horizons".

[3] ICAO, *2013–2028 Global Air Navigation Plan*, Doc 9750-AN/963, 4th edition, 2013.

[4] SESAR, *Step 1 V3 UDPP Validation Report (D67), Optimized Airspace User Operations*, 2015.

[5] https://www.eurocontrol.int/eec/gallery/content/public/documents/other_documents/Air_traffic_conflict_resolution .pdf

[6] B. Antulov-Fantulin, T. Rogošić, B. Juričić, and P. Andraši, "Air traffic controller assessment of the free route airspace implementation within zagreb area control centre," in *Proceedings of the International Scientific Conference Science and Traffic Development-ZIRP*, 2018.

[7] J. K. Kuchar and L. C. Yang, "A Review of Conflict Detection and Resolution Modeling Methods," *IEEE Transactions on Intelligent Transportation Systems*, vol. 1, no. 4, pp. 179–189, 2000.

[8] M. Campo and F. Javier, *The collision avoidance problem. Methods and algorithms [Doctoral dissertation]*, Universidad Rey Juan Carlos, 2010.

[9] O. Rodionova and B. Sridhar, *Efficient Planning of Wind-Optimal Routes in North Atlantic Oceanic Airspace*, 2017.

[10] L. Pallottino, E. M. Feron, and A. Bicchi, "Conflict resolution problems for air traffic management systems solved with mixed integer programming," *IEEE Transactions on Intelligent Transportation Systems*, vol. 3, no. 1, pp. 3–11, 2002.

[11] M. Christodoulou and C. Costoulakis, "Nonlinear mixed integer programming for aircraft collision avoidance in free flight," in *Proceedings of the 12th IEEE Mediterranean Electrotechnical Conference, MELECON 2004*, vol. 1, pp. 327–330, IEEE, May 2004.

[12] A. Vela, S. Solak, W. Singhose, and J. P. Clarke, "A mixed integer program for flight-level assignment and speed control for conflict resolution," in *Proceedings of the 48th IEEE Conference on Decision and Control, 2009 held jointly with the 2009 28th Chinese Control Conference*, pp. 5219–5226, IEEE, 2009.

[13] A. E. Vela, S. Solak, J.-P. B. Clarke, W. E. Singhose, E. R. Barnes, and E. L. Johnson, "Near real-time fuel-optimal en route conflict resolution," *IEEE Transactions on Intelligent Transportation Systems*, vol. 11, no. 4, pp. 826–837, 2010.

[14] A. Alonso-Ayuso, L. F. Escudero, and F. J. Martín-Campo, "Collision avoidance in air traffic management: a mixed-integer linear optimization approach," *IEEE Transactions on Intelligent Transportation Systems*, vol. 12, no. 1, pp. 47–57, 2011.

[15] A. Alonso-Ayuso, L. F. Escudero, P. Olaso, and C. Pizarro, "Conflict avoidance: 0-1 linear models for conflict detection & resolution," *TOP*, vol. 21, no. 3, pp. 485–504, 2013.

[16] S. Cafieri, L. Cellier, F. Messine, and R. Omheni, "Combination of optimal control approaches for aircraft conflict avoidance via velocity regulation," *Optimal Control Applications and Methods*, vol. 39, no. 1, pp. 181–203, 2018.

[17] J. Omer, "A space-discretized mixed-integer linear model for air-conflict resolution with speed and heading maneuvers," *Computers & Operations Research*, vol. 58, pp. 75–86, 2015.

[18] S. Cafieri and D. Rey, "Maximizing the number of conflict-free aircraft using mixed-integer nonlinear programming," *Computers & Operations Research*, vol. 80, pp. 147–158, 2017.

[19] N. Durand, J.-M. Alliot, and J. Noailles, "Automatic aircraft conflict resolution using genetic algorithms," in *Proceedings of the 1996 ACM Symposium on Applied Computing, SAC 1996*, pp. 289–298, ACM, February 1996.

[20] N. Durand and J.-M. Alliot, "Ant Colony Optimization for air traffic conflict resolution," in *Proceedings of the 8th USA/Europe Air Traffic Management Research and Development Seminar, ATM 2009*, pp. 182–187, July 2009.

[21] G. Meng and F. Qi, "Flight conflict resolution for civil aviation based on ant colony optimization," in *Proceedings of the 2012 Fifth International Symposium on Computational Intelligence and Design (ISCID)*, vol. 1, pp. 239–241, IEEE, 2012.

[22] D. Alejo, J. A. Cobano, G. Heredia, and A. Ollero, "Particle swarm optimization for collision-free 4d trajectory planning in unmanned aerial vehicles," in *Proceedings of the 2013 International Conference on Unmanned Aircraft Systems, ICUAS 2013*, pp. 298–307, IEEE, May 2013.

[23] M. Janic, *Air Transport System Analysis and Modelling*, CRC Press, 2014.

[24] J. Carlier, D. Nace, V. Duong, and H. H. Nguyen, "Using disjunctive scheduling for a new sequencing method in multiple-conflicts solving," in *Proceedings of the 2003 IEEE Intelligent Transportation Systems*, vol. 1, pp. 708–714, IEEE, 2003.

[25] C. Sheehan, *Coverage of 2012 European Air Traffic for the Base of Aircraft Data (BADA)-Revision 3.11*, 2007.

[26] J. H. Holland, "Genetic algorithms," *Scientific American*, vol. 267, no. 1, pp. 66–72, 1992.

[27] M. Affenzeller, A. Beham, M. Kofler, G. Kronberger, S. A. Wagner, and S. Winkler, "Metaheuristic optimization," in *Hagenberg Research*, pp. 103–155, Springer, Berlin, Germany, 2009.

[28] F. Glover and M. Laguna, "Tabu search," in *Handbook of Combinatorial Optimization*, pp. 2093–2229, Springer, Boston, MA, USA, 1998.